Langmuir

ARTICLE

pubs.acs.org/Langmuir

Organogels Based on J- and H-Type Aggregates of Amphiphilic Perylenetetracarboxylic Diimides

Haixia Wu,[†] Lin Xue,[†] Yan Shi,[†] Yanli Chen,[‡] and Xiyou Li*[,†]

[†]Key Laboratory of Colloid and Interface Chemistry, Ministry of Education, Department of Chemistry, Shandong University, Jinan, China 250100

[‡]Department of Chemistry, University of Jinan, Jinan, China 250022

Supporting Information

ABSTRACT: Three new perylenetetracarboxylic diimide (PDI) compounds substituted with hydrophobic and/or hydrophilic groups at the two imide nitrogen positions, namely *N*,*N*′-di[*N*-(4-aminophenyl)-3,4,5-tris(2-(2-(2-methoxyethoxy)ethoxy)ethoxy)benzamide]-1,7-di(4-*tert*-butylphenoxy)perylene-3,4;9,10-tetracarboxylic diimide (**1**), *N*,*N*′-di[*N*-amido-3,4,5-tris(2-(2-(2-methoxyethoxy)ethoxy)ethoxy)benzamide]-1,7-di(4-*tert*-butylphenoxy)perylene-3,4;9,10-tetracarboxylic diimide (**2**), and *N*-amido-3,4,5-tris(2-(2-(2-methoxyethoxy)ethoxy)ethoxy)benzamide-*N*′-amido-3,4,5-tris(dodecyloxy)benzamide-1,7-di(4-*tert*-butylphenoxy)perylene-3,4;9,10-tetracarboxylate diimide (**3**), have been designed and prepared. The gelating abilities of them in different solvents have been investigated, and the results indicated that compounds **1** and **3** can form fluorescent gels whereas compound **2** cannot. The properties of the gels of compounds **1** and **3** have been investigated by UV−vis absorption and emission spectra. The results indicate that the gel of compound **1** is composed of H-aggregates, whereas the gel of compound **3** is composed of J-aggregates. The reversible transformation between gel and solution states induced by temperature change is observed. The structure of dried gel has been investigated by X-ray diffraction (XRD) experiments, and the morphology has been measured by atomic force microscopy (AFM). This research revealed successfully the crucial roles of amphiphilic properties and the side-chain conformations in controlling the gelating properties of PDI molecules. This information may be useful for the design of novel organogels based on perylenetetracarboxylic diimides.

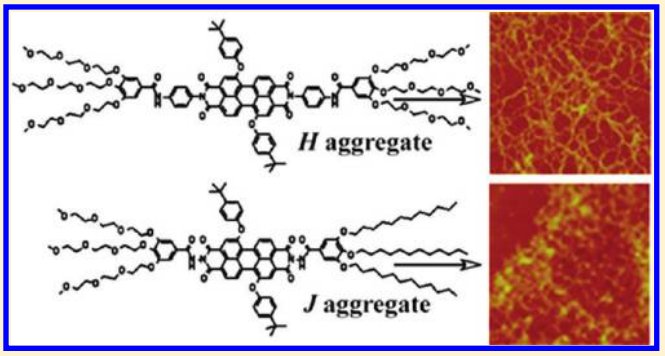

INTRODUCTION

In recent years, organogels have received a great deal of attention as novel materials due to their potential application in many fields, such as templates for mineralization,[1] ion-selective membranes,[2] thermo- and mechanoresponsive sensor materials,[3] and nano- and mesoscopic assemblies with interesting optical and electronic properties.[4−7] In addition, the gel phase is different from either the solid phase or the liquid phase, so it is expected to provide a novel environment for a photochemical or photophysical process.[8]

The formation of organogel is attributed to the molecular self-assembly in solution by noncovalent interactions such as $\pi-\pi$ stacking, hydrogen bonding, metal-ion coordination, dipole−dipole interactions, and other van der Waals interactions. Recently, organogelators based on porphyrins,[4d,6,9] phthalocyanines,[10] and conjugate oligomers[5,11] have been developed. In a recent literature, the first example of a high-aspect-ratio nanofiber hydrogel based on coronene and methyl viologen with charge-transfer interactions in water was prepared by George.[12] However, to date, perylenetetracarboxylic diimide (PDI)-based gels have rarely been reported. Würthner and co-workers reported the first highly fluorescent organogels based on J-aggregates of PDI or ureacontaining PDIs.[13,14] From the same group, a novel n-type semiconducting PDI compound was developed, which contains six long hydrophobic alkyl chains and exhibits excellent gelating capabilities and good charge carrier mobilities.[15] Shinkai and co-workers prepared several gelators by connecting cholesterol groups to the imide positions of PDI ring. The resulted compounds can form mixed gel in a mixed solvent of *p*-xylene and 1-propanol. More interestingly, efficient energy transfer can be observed between the different components of the mixed gel.[8b] Recently, Rybtchinski has prepared an amphiphilic PDI compound by connecting hydrophilic chains at the 1,7-positions of PDI ring. The new compound can form supramolecular gel in water/THF mixtures with multiple stimuli responsiveness and photofunction.[16] Up to now, the effects of molecular structure on the gelating capabilities of PDI compounds are far from fully understood.

In the present work, we will report on the design and synthesis of three novel PDI compounds; two of them are connected with hydrophilic side chains, and the other one substituted with both

Received: December 8, 2010
Revised: January 12, 2011
Published: February 14, 2011

Scheme 1. Structures of Compounds 1−3

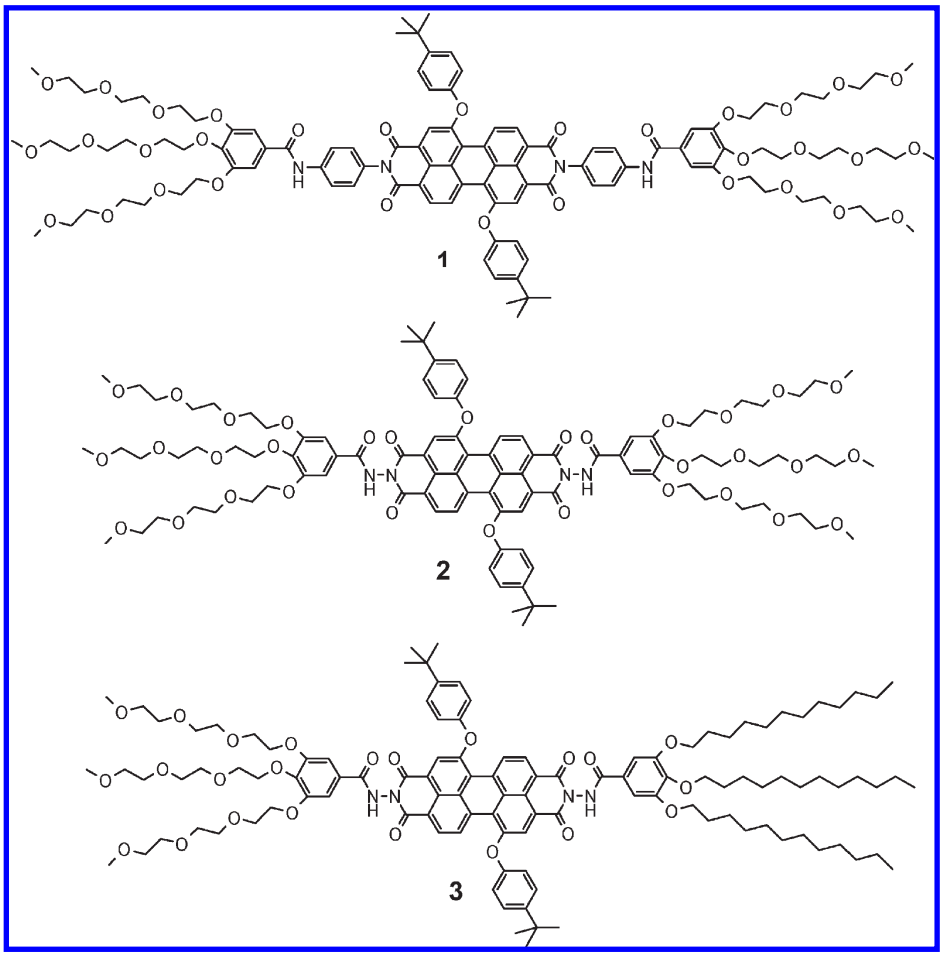

hydrophobic and hydrophilic side chains. Comparative studies on their gelating properties revealed that the amphiphilic properties and $\pi-\pi$ stacking have large effects on the gelating process as well as the gel structure. The information provided here maybe useful for the design of novel organogels based on PDI compounds.

RESULTS AND DISCUSSION

Molecular Design and Synthesis. The structures of the PDIs (**1**−**3**) are shown in Scheme 1. The synthetic procedures and structure characterization are described in detail in the Supporting Information. To keep a good solubility of PDIs in conventional organic solvents, we chose polyoxyethylene as the hydrophilic tail and the PDI mother ring with two hydrophobic phenoxyl groups at 1,7 positions as the hydrophobic head. Additionally, the 1,7-disubstituted PDI rings have very strong $\pi-\pi$ interactions, which will promote the gelating properties of the compounds as reported in the literature.[8b,13−15]

Gelating Properties. Compound **1** has a good solubility in methanol, ethanol, and toluene, whereas it is virtually insoluble in hexane. Compound **1** does not form gel in any pure conventional organic solvents tested, but it can form an opaque gel (**I**) in a mixed solvent of ethanol and hexane (1:1 v/v). The minimum gelating concentration is 3.2 mM. Moreover, compound **1** can form a transparent gel (**II**) in a mixed solvent of toluene and methanol (1:1 v/v), but a higher gelating concentration is needed (7.8 mM). The formation of gel was defined by the "stable-to-inversion of a vial" method. Figure 1A,B shows the photographs of the gels.

To our surprise, compound **2** does not gelate at all. Numerous experiments in pure or mixed solvents lead to either transparent solution or precipitate. Because compound **2** has same hydrophobic and hydrophilic groups, the difference between their gelating properties can only be ascribed to the difference on the linkage between the hydrophobic head and hydrophilic tail. The optimized molecular structures of compounds **1**−**3** calculated with MM^{+} molecular mechanical modeling are shown in Figure 2. It can be found that the hydrophilic unit and the PDI ring in compound **1** take a coplanar conformation. But in compound **2**, the hydrophobic unit is directly linked through N−N bond with the PDI ring; this has forced the hydrophilic units bending from the plane of the PDI ring, and a coplanar conformation cannot be achieved. Therefore, the additional phenyl rings made the molecular structure of compound **1** more planar than **2**, which favor the $\pi-\pi$ stacking between molecules. It is widely recognized that a prerequisite for the formation of organic gel is that gelator molecules self-assembled into long linear aggregates. The larger $\pi-\pi$ interaction between the molecules of compound **1** relative to that of compound **2** leads to the results that compound **1** can form gel whereas compound **2** cannot.

dx.doi.org/10.1021/la104888p |*Langmuir* 2011, 27, 3074–3082

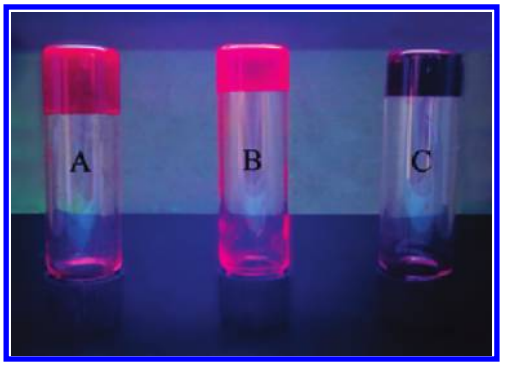

Figure 1. Photographs of gels **I** (A), **II** (B), and **III** (C) under a UV lamp (365 nm). The minimum concentration for gelator is 3.2, 7.8, and 5.0 mM, respectively.

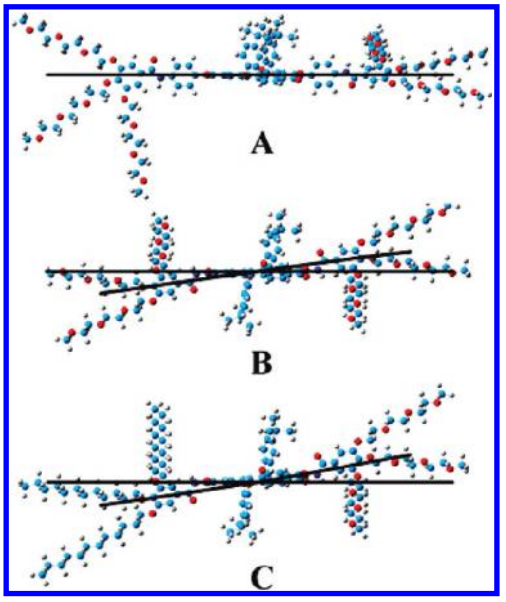

Figure 2. Optimized molecular structures of compounds **1** (A), **2** (B), and **3** (C).

Compound **3** contains a hydrophobic tail and a hydrophilic tail. It can form an opaque gel (**III**) in hexane. Compared with that of compound **2**, compound **3** has similar nonplanar molecular structure except for three long hydrophobic alkyl chains. This result indicates that the hydrophobic interactions between the long alky chains play an important role on the gelating process. The formation of fluorescent organogel of compound **3** is the result of the cooperation between intermolecular $\pi-\pi$ interaction and the hydrophobic interaction.

UV−vis Absorption and Fluorescence Spectra. UV−vis absorption and fluorescence spectra of PDIs are sensitive to the interchromophore distance and orientation[17,18] and, therefore, have been widely used to study their $\pi-\pi$ stacking.[19−21] The absorption and fluorescent spectra of compound **1** in chloroform and a dilute gel **I** are shown in Figure 3, and the spectral parameters are summarized in Table 1. The absorption spectrum of compound **1** in chloroform exhibits typical spectroscopic features that are expected for monomeric diphenoxy-substituted PDI chromophores.[22] The absorption maxima at 550 nm is attributed to the 0−0 transition, whereas the small shoulder at about 515 nm can be assigned to the 0−1 transition. The

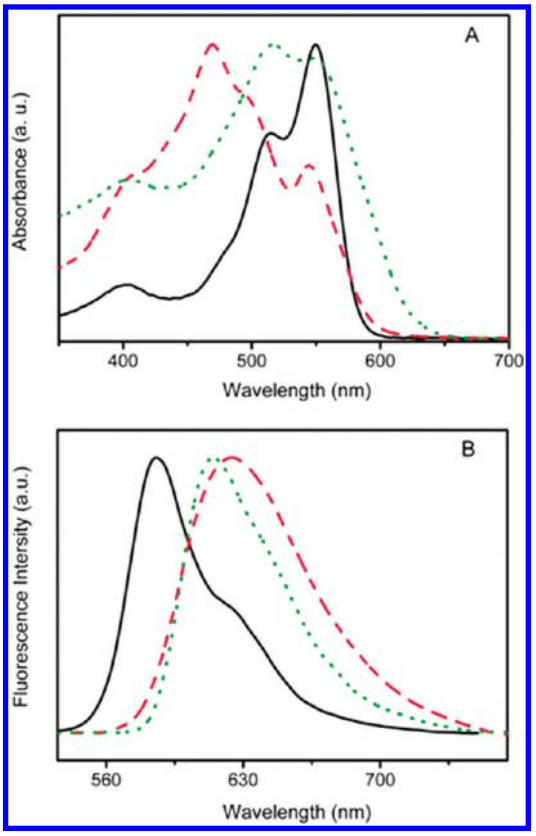

Figure 3. UV/vis (A) and fluorescence (B) spectra (excited at 450 nm) of compound **1** in $CHCl_3$ (solid): a dilute gel **I** (dashed) and gel **II** (dotted).

Table 1. Absorption and Emission Parameters of Compounds 1 and 3 in Solution or in Gel

	λ_{max}^{abs} (nm)	λ_{max}^{flu} (nm)	Φ_f (%)[a]
gel **I**	470	624	0.18
gel **II**	515	614	0.15
compound **1** in $CHCl_3$	550	585	58.20
gel **III**	541	690	2.31
compound **3** in hexane	503	680	0.87
compound **3** in $CHCl_3$	550	585	74.18

[a] With *N*,*N*-dihexyl-1,7-di(4-*tert*-butyl)phenoxyperylene-3,4;9,10-tetracarboxylate diimide (Φ_f = 100%) as standard.

emission spectrum with a peak maximum at 585 nm is the mirror image of the absorption band. However, the maximum absorption band of gel **I** strongly blue-shifted for 80 nm (470 nm) compared with the monomer's absorption band, which indicates very strong ground state interactions between the neighboring molecules in gel **I**. Similarly, the emission maximum of the fluorescence spectrum red-shifted distinctively to 624 nm relative to that of the monomer, which can be assigned to an "excimer-like" state of PDI. This observation suggests that the molecules of compound **1** in gel **I** interact with each other not only on the ground states but also on the excited states. The absorption and fluorescence changes of compound **1** relative to those in chloroform indicate the formation of H-type aggregates during the gelating process in the mixed solvent of hexane and ethanol (1:1 v/v).[23] It is worth noting that the blue shift (80 nm) on the maximum absorption band of gel **I** is much larger than that

reported previously for other H-aggregates of PDIs.[13,21,22a,24] For example, our previously reported cyclic PDI dimer with rigid structure blue-shifted for only 38 nm relative to the monomer.[23a] As reported in the literature, PDIs with different substituents at imide positions could pack in different patterns in crystals and present different absorption spectra due to the different interactions between the adjacent molecules.[25] Slippages along the longitudinal or transverse direction cause significant red-shifted absorption maximum, whereas the in-plane torsion between the adjacent PDI rings induces significant blue shift on the absorption peaks. Therefore, it is reasonable to ascribe partially the extra large blue shift on absorption spectra to small in-plane torsion and very small slippages along the longitudinal or transverse direction between the adjacent molecules of compound **1** in gel **I**. Another reason that causes the extra large blue shift on the absorption spectra of gel **I** might be the small interplanar distance which caused large ground state interactions between the adjacent molecules.[26] The absorption spectrum of gel **II** shows a maximum absorption peak at 515 nm, which blue shift for about 35 nm relative to that of monomeric PDI. This is a typical absorption spectrum of face-to-face stacked PDI aggregates.[22a,23a,26] The fluorescence spectrum of gel **II** shows excimer-like emission with a maximum at 614 nm, which red-shifted for about 30 nm relative to that of monomer and blue-shifted 10 nm relative to that of gel **I**. Both the absorption and emission spectra of gel **II** suggest that the stacking model of the molecules of compound **1** in gels **I** and **II** are both face-to-face stacking, but with difference on their microstructure. The opaque to transparency change from **I** to **II** maybe caused by the solubility of compound **1** in the different mixed solvents. The low solubility of compound **1** in hexane/ethanol induces the formation of large aggregates and opaque gel **I**, while the higher solubility of compound **1** in toluene/methanol leads to the formation of transparency gel **II**.[27]

The absorption and fluorescence spectra of compound **3** in homogeneous solutions and a dilute gel **III** are shown in Figure 4. The maximum absorption band of compound **3** in hexane blue-shifted for about 47 nm (503 nm) relative to that in $CHCl_3$. A similar blue shift can be observed when the concentration of compound **3** decrease to as low as 10^{-7} mol L^{-1}. This result implies that compound **3** forms molecular aggregates with face-to-face stacked structure even in very dilute solution of hexane.[22a,23a] The fluorescence spectrum of compound **3** in hexane presents maximum emission at about 680 nm, which is a typical emission of PDI excimer-like state and suggests again that compound **3** stacks in a face-to-face way and forms H-aggregates in hexane.

The absorption spectrum of dilute gel **III** presents a maximum absorption at about 540 nm and a pronounced new band at 644 nm. The spectral characteristics are typical sign of effective $\pi-\pi$ interaction with coplanar configuration of molecular stacking,[25,28] indicating the formation of J-aggregates in gel **III**.[29] The fluorescence spectrum of gel **III** shows broad emission band in the range of 620−770 nm with a maximum emission at about 690 nm, which is almost identical to that of compound **3** in hexane except a small red shift (10 nm) on the emission maximum. It is surprising because their absorption spectra are significantly different from each other. To reveal the origin of the fluorescence of compound **3** in hexane and in gel **III**, excitation spectra are recorded (Figure S1 in Supporting Information). It can be found that the excitation spectra resembled their absorption spectra in shape and revealed that the fluorescence of

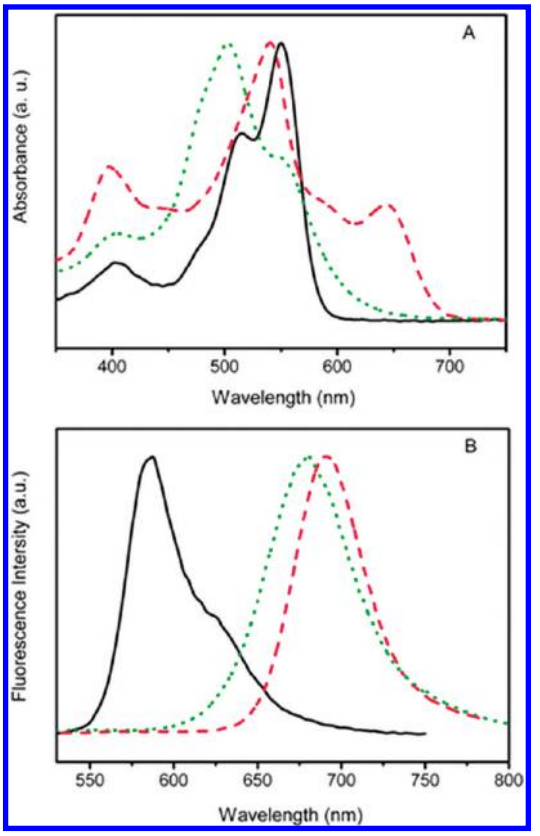

Figure 4. UV/vis (A) and fluorescence (B) spectra (excited at 450 nm) of compound **3** in $CHCl_3$ (solid), hexane (dotted), and a dilute gel **III** in gelling solvent hexane (dashed).

compound **3** in hexane and in gel **III** originated from different aggregated states. The fluorescence of compound **3** in hexane is assigned to the H-type aggregates, which show excimer-like emission,[22a,23a,30] while the fluorescence of gel **III** can be attributed to the J-type aggregates (Figure S4).

The exchange between H- and J-aggregates leads to significant change on the color of the solution and can be identified by naked eye. The color of the H-aggregates of compound **3** in hexane is red, but that of gel **III** is black. Similar color change has been reported previously by Mizuguchi for a thin solid film of nonsubstituted PDI pigment. The color change upon thermal treatment was explained in terms of a transition from a less ordered aggregate state to a highly ordered crystalline state.[31] Recently, a black gel based on a nonsubstituted PDI was prepared by Würthner and co-workers.[32] The black color was ascribed to the formation of J-aggregates of PDIs in gel with pronounced longitudinal displacement.[25,33] It is worth noting that the significant color change we observed for the aggregates of compound **3** before and after gel formation is never been reported for a PDI with bay substituents.

The fluorescence quantum yields are calculated with *N,N*-dihexyl-1,7-di(4-*tert*-butyl)phenoxyperylene-3,4;9,10-tetracarboxylate diimide (Φ_f = 100%) as standard,[34] and the results are summarized in Table 1. In pure chloroform, both compound **1** and compound **3** presented as monomer and therefore are highly fluorescent. Their fluorescence quantum yields are measured to be 58.20% and 74.18%, respectively. But in gels, their fluorescence quantum yields reduced significantly to 0.18%, 0.15%, and 2.31% for gel **I**, gel **II**, and gel **III**, respectively. This can be

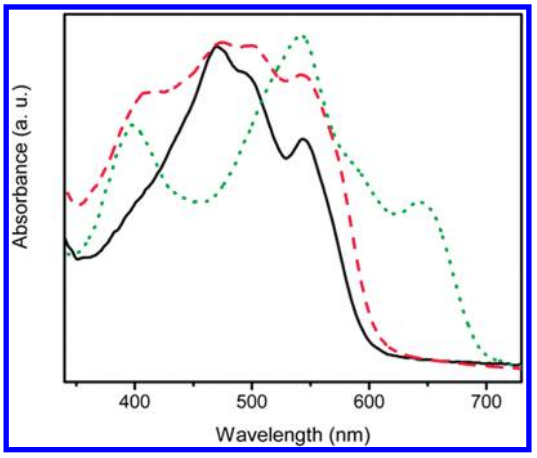

Figure 5. UV/vis spectra of solid gels of **I** (solid), **II** (dashed), and **III** (dotted).

ascribed to the formation of molecular aggregates during gelating process. The fluorescence quantum yield of compound **3** in hexane is much smaller than that of gel **III**, which is rational because compound **3** in hexane forms H-aggregates while in gel **III** is J-aggregates as revealed by the absorption and fluorescence spectra.[13] This result reveals again that the emission from compound **3** in hexane and gel **III** are virtually different, corresponding well with the results of excitation spectra.

In addition, the UV−vis absorption spectra of the thin films of the gels prepared by daubing the gel on a glass surface are also recorded (Figure 5). We found that their spectroscopic features of gel **I** and gel **III** are similar to that recorded for suspensions, implying that the packing models of the PDI molecules in thin solid film are same as that in dilute suspension. But the absorbance spectrum of solid gel **II** shown an obvious band broadening after evaporation of the solvents, which maybe attributed to the effect of the closely compacting in the dried gel.[35,36]

Temperature-Dependent Absorption Spectra. To investigate the effects of temperature on the properties of the gels, we carried out temperature-dependent absorption measurements on the gels. Absorption spectral changes of gel **I** in a mixed solvent of hexane and ethanol (1:1 v/v) at variable temperature between 20 and 65 °C are shown in Figure 6. Along with temperature increase, the sharp absorption band at 470 nm, a sign of face-to-face stacked molecular aggregates, disappears gradually while the absorption of monomeric species at longer wavelength increases synchronously. Gel **I** changes from a gel state to a transparent solution at the same time. This observation reveals that temperature rise has broken the molecular aggregates of PDI in gel **I** and thus destroyed the gel structure. Moreover, the changes on the absorption spectra are reversible after decrease the temperature subsequently (Figure S2A). These thermoreversible spectral changes clearly testify that the strong $\pi-\pi$ interaction between the face-to-face stacked PDI rings dominating the gelating process of compound **1**. Gel **II** show same thermoreversible spectral changes as gel **I**.

The temperature-dependent UV−vis absorption spectra for gel **III** in hexane are shown in Figure 7. The band centered at about 644 nm together with the sharp absorption maximum at 541 nm disappeared gradually along with temperature increase. The face-to-face dimeric species was formed at the same time as revealed by the formation of the dimer's absorption band at about 503 nm. It is worth noting that, at low temperature, such as below

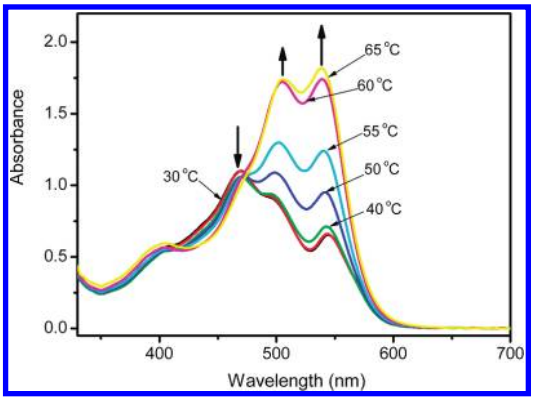

Figure 6. Temperature-dependent absorption spectra of a dilute gel of **I**. The arrows indicate spectral changes with increasing temperature.

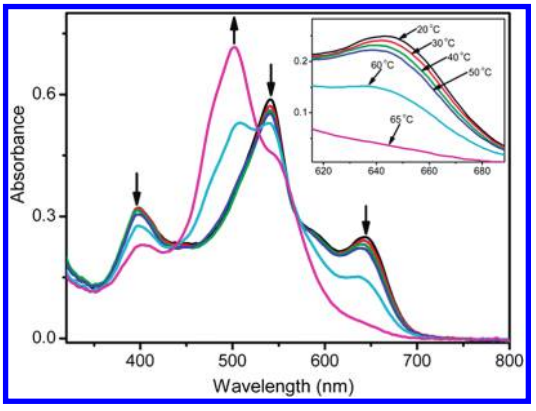

Figure 7. Temperature-dependent absorption spectra of a dilute gel of **III**. The arrows indicate spectral changes with increasing temperature.

50 °C, the gel is stable and does not show significant changes on the absorption spectra along with temperature increase. Upon cooling, the dimer's absorption did not change distinctively except a small increase on the absorption intensity, and the testing sample kept as a transparent solution (Figure S2B). This result seems indicate that gelating of compound **3** in hexane is not a thermally reversible process. But the features of the gel's absorption recovered after the solution was stored at 20 °C for 10 days, and gel **III** formed again. These results clearly indicate that H-aggregates with face-to-face configuration of compound **3** in hexane is a kinetics controlled product while the J-aggregates is a thermodynamically controlled product.

X-ray Diffraction Patterns of the Gels. The internal structures of dried gels were further investigated by X-ray diffraction (XRD) experiments. The diffraction patterns of gels **I**, **II**, and **III** are compared in Figure 8. The most significant difference between the diffraction patterns of gels **I** and **II** is observed in the 2θ range of 15°−25°, where the diffraction pattern of gel **II** shows a broad peak while that of gel **I** does not. The broad peak at this range is normally ascribed to the formation of liquidlike order of long alky chains.[37] These results indicate that the alkyl chains in gel **II** packed with higher order than that in gel **I**. This is likely caused by the different solubility of compound **1** in the gelated solvents. Because compound **1** cannot dissolve in hexane, the solubility of it in the mixed solvent of hexane/ethanol is small. The long hydrophilic alkyl chains in this poor solvent cannot take an extended conformation but a folded and tangled

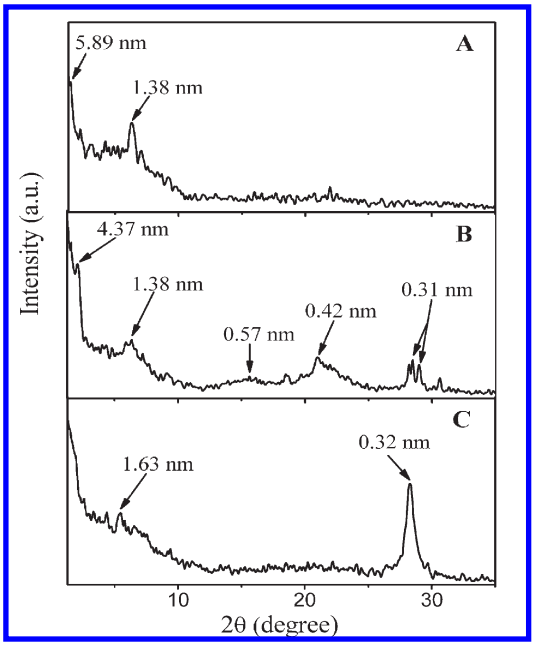

Figure 8. XRD patterns for dry gels of **I** (A), **II** (B), and **III** (C).

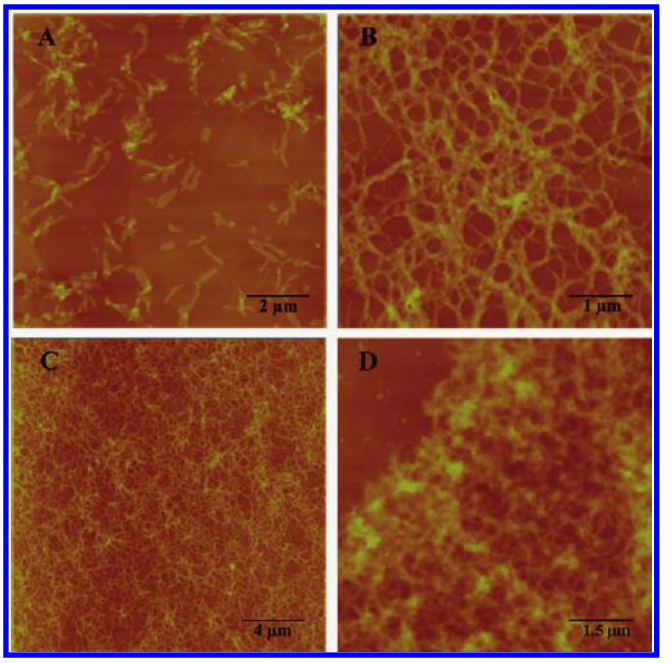

Figure 9. AFM images of gels **I** (A), **II** (B, C), and **III** (D) on silicon surfaces.

conformation instead. Consequently, the liquidlike order of long alkyl chains in gel **I** cannot be found. Contrarily, because compound **1** can dissolve in both toluene and methanol, the solubility of compound **1** in the mixed solvent of toluene and methanol is large, and therefore the hydrophilic chains in this mixed solvent can take an extended conformation. As a result, the long alkyl chains can pack with high order in gel **II**.

In the diffraction pattern of gel **II**, two diffraction peaks at about $2\theta = 28.5°$ and 28.9° can be observed, which corresponds to the d space of 0.31 nm and can be assigned to the interplanar space between the face-to-face stacked aromatic rings based on $\pi-\pi$ interaction.[25,38] The appearance of these peaks indicates that the PDI and other aromatic units in gel **II** stacked with high order. However, this peak does not present in the diffraction pattern of gel **I**, suggesting that the PDI as well as other aromatic parts of compound **1** do not stack with high order in this gel. This result is in line with the in-plane torsion conformation between the adjacent molecules in gel **I** as suggested by the absorption spectra.

In the low angle region of the diffraction pattern of gel **I**, a peak at $2\theta = 1.50°$ corresponding to a d space of 5.89 nm is observed. This value is close to the length of the molecule along the longitudinal (5.80 nm) calculated from the energy-optimized conformation of the molecule by MM^+ molecular mechanical modeling (Figure S3, Supporting Information). A similar diffraction peak at $2\theta = 2.02°$, corresponding to a d space of 4.37 nm, is observed in the diffraction pattern of gel **II**. This value is significantly smaller than the length of the molecule along the longitudinal (5.80 nm), which is likely caused by the effective chain interdigitation between the adjacent molecules in gel **II**.[39]

In the low angle region, both gel **I** and **II** show a strong and broad diffraction peak at about $2\theta = 6.38°$, which corresponds to a d space of about 1.38 nm. This value is approximately equal to that of the thickness of five molecules stacked in a face-to-face way with an interplanar space of 0.31 nm, which suggests that in a unit cell of the periodic structure contains five molecules.

The diffraction pattern of gel **III** presents a broad peak at about $2\theta = 28.2°$, corresponding to a d space of 0.32 nm as shown in Figure 8C, which can be assigned to the $\pi-\pi$ stacking in gel **III**. No broad diffraction peak appears in the 2θ region of 15°−25°, suggesting that both hydrophilic and hydrophobic alkyl chains of compound **3** in gel **III** cannot form liquidlike ordered structure. Similar to that observed for gels **I** and **II**, a broad diffraction peak at $2\theta = 5.43°$, corresponding to a d space of 1.63 nm, was observed in the low angle region of the diffraction pattern of gel **III**. This value is approximately equal to that of the thickness of six molecules stacked in a face-to-face way with an interplanar space of 0.32 nm. This result suggests π systems in gel **III** packing more orderly than that in gels **I** and **II**.

Morphology of the Gels. The morphology of the gels was examined by atomic force microscopy (AFM) via the tapping model (Figure 9). As can be seen from Figure 9A, depending mainly on the intermolecular $\pi-\pi$ interaction, compound **1** in gel **I** self-assembles into beltlike aggregates. However, as shown in Figures 9B,C, network nanostructures are formed in gel **II**, which maybe resulted from the cooperation of intermolecular $\pi-\pi$ interaction as well as hydrophilic chain interactions. As mentioned above, the hydrophilic chains of compound **1** in the mixed solvent of hexane/ethanol tangle or bend due to the low solubility as revealed by the absorption spectra and the XRD experiments. This has hindered the interdigitations between the hydrophilic chains of different molecules, and therefore the molecular aggregates cannot grow along the direction of the hydrophilic chain extension. However, in the mixed solvent of toluene and methanol, the hydrophilic chains take extended conformations and efficient chain interdigitation can be achieved, and therefore the aggregates can grow along the direction of chain extension and form long fibers and networks. The above results confirmed the effects of the solvents on tuning the intermolecular interaction and in turn the molecular packing mode in aggregates during the gelating process.[40]

For compound **3**, because of the presence of extra hydrophobic alkyl chains, the interaction between the side chains of adjacent molecules are therefore composed of two parts, i.e.,

dx.doi.org/10.1021/la104888p |*Langmuir* 2011, 27, 3074–3082

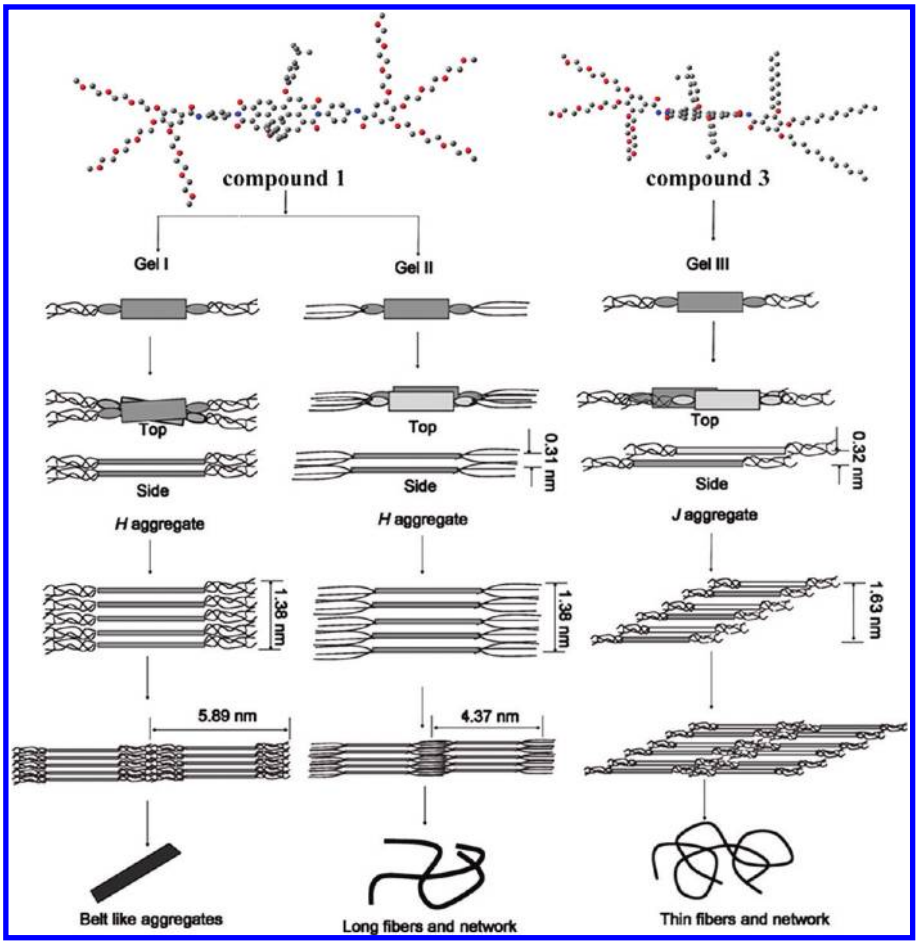

Figure 10. Schematic aggregation processes of compounds **1** and **3** in gels **I**, **II**, and **III**.

hydrophobic interactions and hydrophilic interactions. This actually makes the interactions more directional and block the unlimit growth of the aggregates along the direction of chain extension. This is why compound **3** forms very thin filaments, which further entangle together as shown in Figure 9D.

On the basis of the results of XRD, spectroscopic experiments, and morphology examination, we can draw a speculated microstructure for the molecular aggregates in gel **I**, **II**, and **III**, respectively (Figure 10). For compound **1** in gel **I**, the molecules stacked in face-to-face way with small in-plane torsion. Because of the tangling or bending of long alkyl hydrophilic chains, the side chains cannot pack with high order and therefore cannot provide significant help on the growth of molecular aggregates. The molecular aggregates in gel **I** can only grow along the direction of $\pi-\pi$ stacking. Because lack of help from other intermolecular interactions, the molecular aggregates in gel **I** cannot grow into long fibers and form network as that observed for gel **II**. In gel **II**, molecules of compound **1** stacked similarly with that in gel **I** driven by the strong $\pi-\pi$ interaction. Because of the presence of effective chain interdigitation, which provides extra driving force for the molecular aggregation, the small molecular aggregates of compound **1** in gel **II** therefore can grow into long fibers and network with ease. In gel **III**, the molecules of compound **3** stacked in a face-to-face way with large slippages along the longitudinal direction to form linear aggregates. Because of the selection between hydrophobic and hydrophilic interactions between the side chains, the aggregates grow in a more directional way, and accordingly only very thin fibers are formed.

CONCLUSION

Three new PDI derivatives connected with hydrophilic and/or hydrophobic side chains at imide nitrogen positions were synthesized. Compound **1** with hydrophilic groups at imide nitrogen positions linked by phenyl ring can form different gels in different solvents. In the mixed solvent of hexane and ethanol, an opaque gel was formed due to the low solubility of compound **1** in this mixed solvent. The hydrophilic chains of compound **1** in this gel cannot pack with high order due to the chain tangling or bending, which in turn to affect the stacking of the PDI units. In the mixed solvent of toluene and methanol, a transparent gel was formed probably because of the large solubility of compound **1** in this mixed solvent. The hydrophilic chains of compound **1** in this mixed solvent could take extended conformation and achieve effective chain interdigitations. The significant hydrophilic chain interactions play an important role in the formation of long fibers and network during the gelating process. Compound **3** with both hydrophobic and hydrophilic chains can form gel in conventional organic solvents more easily than compound **1**, which suggests that amphiphilic properties are very important for a gelator. Introduction of hydrophobic long alkyl chains has actually made the side-chain interactions more directional because side chains of one molecule can only interact with the same side chains of next molecule. The result is compound **3** can only form very thin

dx.doi.org/10.1021/la104888p |*Langmuir* 2011, 27, 3074–3082

filaments during the gelating process. We believe that the information we got will be helpful for the design of novel organogels.

EXPERIMENTAL SECTION

^{1}H NMR spectra were recorded at 300 MHz with the solvent peak as the internal standard (in $CDCl_3$). Electronic absorption spectra were recorded on a Hitachi 4100 spectrometer. Fluorescence spectra were measured on an ISS K2 system. MALDI-TOF mass spectra were taken on a Bruker BIFLEX III mass spectrometer with α-cyano-4-hydroxycinnamic acid as the matrix. The low-angle X-ray diffraction (LAXD) experiment was carried out on a Rigaku D/max-γ B X-ray diffractometer. The morphology of nanostructures on Si was studied in air by use of a Veeco multimode atomic force microscope (AFM) in tapping mode.

ASSOCIATED CONTENT

Supporting Information. Details for synthetic procedure, ^{1}H NMR and MALDI-TOF mass spectroscopy results, excitation spectra of compound **3** in homogeneous solutions and gel **III**, temperature-dependent absorption spectra of gels **I** and **III**, optimized molecular structures of PDI **1** and PDI **3**, and a comparison of the fluorescence spectra of gel **III** with that of monomeric compound **3**. This material is available free of charge via the Internet at http://pubs.acs.org.

AUTHOR INFORMATION

Corresponding Author
*E-mail: xiyouli@sdu.edu.cn.

ACKNOWLEDGMENT

Financial support from the Natural Science Foundation of China (20771066 and 20871055), Ministry of Education of China, and Shandong University is gratefully acknowledged.

REFERENCES

(1) (a) Fujita, N.; Asai, M.; Yamashita, T.; Shinkai, S. *J. Mater. Chem.* **2004**, *14*, 2106–2114. (b) Numata, M.; Sugiyasu, K.; Hasegawa, T.; Shinkai, S. *Angew. Chem., Int. Ed.* **2004**, *43*, 3279–3283.

(2) Beginn, U.; Möller, M. In *Supramolecular Materials and Technologies*; Reinholdt, D. N., Ed.; Wiley & Sons: Chichester, 1999; pp 89−176.

(3) Beck, J. B.; Rowan, S. J. *J. Am. Chem. Soc.* **2003**, *125*, 13922–13923.

(4) (a) van Esch, J. H.; Feringa, B. L. *Angew. Chem., Int. Ed.* **2000**, *39*, 2263–2266. (b) Schoonbeek, F. S.; van Esch, J. H.; Wegewijs, B.; Rep, D. B. A.; de Haas, M. P.; Klapwijk, T. M.; Kellogg, R. M.; Feringa, B. L. *Angew. Chem., Int. Ed.* **1999**, *38*, 1393–1397. (c) Schoonbeek, F. S.; van Esch, J. H.; Hulst, R.; Kellogg, R. M.; Feringa, B. L. *Chem.—Eur. J.* **2000**, *6*, 2633–2643. (d) Shirakawa, M.; Kawano, S.-i.; Fujita, N.; Sada, K.; Shinkai, S. *J. Org. Chem.* **2003**, *68*, 5037–5044. (e) de Jong, J. J. D.; Lucas, L. N.; Kellogg, R. M.; van Esch, J. H.; Feringa, B. L. *Science* **2004**, *304*, 278–281.

(5) Ajayaghosh, A.; George, S. J. *J. Am. Chem. Soc.* **2001**, *123*, 5148–5149.

(6) Tamaru, S.-i.; Uchino, S.-y.; Takeuchi, M.; Ikeda, M.; Hatano, T.; Shinkai, S. *Tetrahedron Lett.* **2002**, *43*, 3751–3755.

(7) Placin, F.; Desvergne, J.-P.; Lassegues, J.-C. *Chem. Mater.* **2001**, *13*, 117–121.

(8) (a) Ajayaghosh, A.; George, S. J.; Praveen, V. K. *Angew. Chem., Int. Ed.* **2003**, *42*, 332–335. (b) Sugiyasu, K. S.; Fujita, N.; Shinkai, S. *Angew. Chem., Int. Ed.* **2004**, *43*, 1229–1232.

(9) (a) Dammer, C.; Maldivi, P.; Terech, P.; Guenet, J.-M. *Langmuir* **1995**, *11*, 1500–1506. (b) Sagawa, T.; Fukugawa, S.; Yamada, T.; Ihara, H. *Langmuir* **2002**, *18*, 7223–7228. (c) Tamaru, S.-i; Nakamura, M.; Takeuchi, M.; Shinkai, S. *Org. Lett.* **2001**, *3*, 3631–3634.

(10) (a) Van Nostrum, C. F.; Picken, S.; Schouten, A.-J.; Nolte, R. J. M. *J. Am. Chem. Soc.* **1995**, *117*, 9957–9965. (b) Engelkamp, H.; Middelbeek, S.; Nolte, R. J. M. *Science* **1999**, *284*, 785–788.

(11) Schoonbeek, F. S.; van Esch, J. H.; Wegewijs, B.; Rep, D. B. A.; de Haas, M. P.; Klapwijk, T. M.; Kellogg, R. M.; Feringa, B. L. *Angew. Chem.* **1999**, *111*, 1486–1490.

(12) Venkata, R. K.; Jayaramulu, K.; Maji, T. K.; George, S. J. *Angew. Chem., Int. Ed.* **2010**, *122*, 4314–4318.

(13) Li, X.-Q.; Zhang, X.; Ghosh, S.; Würthner, F. *Chem.—Eur. J.* **2008**, *14*, 8074–8078.

(14) Würthner, F.; Hanke, B.; Lysetska, M.; Lambright, G.; Harms, G. S. *Org. Lett.* **2005**, *7*, 967–970.

(15) Li, X.-Q.; Stepanenko, V.; Chen, Z.; Prins, P.; Siebbeles, L. D. A.; Würthner, F. *Chem. Commun.* **2006**, 3871–3873.

(16) Krieg, E.; Shirman, E.; Weissman, H.; Shimoni, E.; Wolf, S. G.; Pinkas, I.; Rybtchinski, B. *J. Am. Chem. Soc.* **2009**, *131*, 14365–14373.

(17) Kazmaier, P. M.; Hoffmann, R. *J. Am. Chem. Soc.* **1994**, *116*, 9684–9691.

(18) Giaimo, J. M.; Lockard, J. V.; Sinks, L. E.; Scott, A. M.; Wilson, T. M.; Wasielewski, M. R. *J. Phys. Chem. A* **2008**, *112*, 2322–2330.

(19) Wang, W.; Li, L.-S.; Helms, G.; Zhou, H.-H.; Li, A. D. Q. *J. Am. Chem. Soc.* **2003**, *125*, 1120–1121.

(20) Balakrishnan, K.; Datar, A.; Oitker, R.; Chen, H.; Zuo, J.; Zang, L. *J. Am. Chem. Soc.* **2005**, *127*, 10496–10497.

(21) Balakrishnan, K.; Datar, A.; Naddo, T.; Huang, J.; Oitker, R.; Yen, M.; Zhao, J.; Zang, L. *J. Am. Chem. Soc.* **2006**, *128*, 7390–7398.

(22) (a) Wang, Y.; Chen, Y.; Li, R.; Wang, S.; Su, W.; Ma, P.; Wasielewski, M. R.; Li, X.; Jiang, J. *Langmuir* **2007**, *23*, 5836–5842. (b) Zhao, C.; Zhang, Y.; Li, R.; Li, X.; Jiang, J. *J. Org. Chem.* **2007**, *72*, 2402–2410.

(23) (a) Feng, J.; Zhang, Y.; Zhao, C.; Li, R.; Xu, W.; Li, X.; Jiang, J. *Chem.—Eur. J.* **2008**, *14*, 7000–7010. (b) Giaimo, J. M.; Gusev, A. V.; Wasielewski, M. R. *J. Am. Chem. Soc.* **2002**, *124*, 8530–8531.

(24) Che, Y.; Datar, A.; Balakrishnan, K.; Zang, L. *J. Am. Chem. Soc.* **2007**, *129*, 7234–7235.

(25) Klebe, G.; Graser, F.; Hadicke, E.; Berndt, J. *Acta Crystallogr.* **1989**, *B45*, 69–77.

(26) Clark, A. E.; Qin, C.; Li, A. D. Q. *J. Am. Chem. Soc.* **2007**, *129*, 7586–7595.

(27) Weng, W.; Li, Z.; Jamieson, A. M.; Rowan, S. J. *Macromolecules* **2009**, *42*, 236–246.

(28) (a) Würthner, F. *Chem. Commun.* **2004**, 1564–1579. (b) Hadicke, E. H.; Graser, F. *Acta Crystallogr.* **1986**, *C42*, 189–195.

(29) (a) van Herrikhuyzen, J.; Syamakumari, A.; Schenning, A. P. H. J.; Meijer, E. W. *J. Am. Chem. Soc.* **2004**, *126*, 10021–10027. (b) Jonkheijm, P.; Stutzmann, N.; Chen, Z.; de Leeuw, D. M.; Meijer, E. W.; Schenning, A. P. H. J.; Würthner, F. *J. Am. Chem. Soc.* **2006**, *128*, 9535–9540.

(30) (a) van der Boom, T.; Hayes, R. T.; Zhao, Y.; Bushard, P. J.; Weiss, E. A.; Wasielewski, M. R. *J. Am. Chem. Soc.* **2002**, *124*, 9582–9590. (b) Kasha, M.; Rawls, H. R.; El-Bayoumi, M. A. *Pure Appl. Chem.* **1965**, *11*, 371–392. (c) Ahren, M. J.; Sinks, L. E.; Rybtchinski, B.; Liu, W.; Jones, B. A.; Giaimo, J. M.; Gusev, A. V.; Goshe, A.; Tiede, D. M.; Wasielewki, M. R. *J. Am. Chem. Soc.* **2004**, *126*, 8284–8294.

(31) Mizuguchi, J. *J. Appl. Phys.* **1998**, *84*, 4479–4486.

(32) Würthner, F.; Bauer, C.; Stepanenko, V.; Yagai, S. *Adv. Mater.* **2008**, *20*, 1695–1698.

(33) Graser, F.; Hädicke, E. *Liebigs Ann. Chem.* **1984**, 483–494.

(34) Chao, C.-C.; Leung, M.-K.; Su, Y. O.; Chiu, K.-Y.; Lin, T.-H.; Shieh, S.-J.; Lin, S.-C. *J. Org. Chem.* **2005**, *70*, 4323–4331.

(35) Chen, Y.; Kong, Y.; Wang, Y.; Ma, P.; Bao, M.; Li, X. *J. Colloid Interface Sci.* **2009**, *330*, 421–427.

(36) Su, W.; Zhang, Y.; Zhao, Ch.; Li, X.; Jiang, J. *ChemPhysChem* **2007**, *8*, 1857–1862.

(37) Würthner, F.; Thalacker, C.; Diele, S.; Tschierske, C. *Chem.—Eur. J.* **2001**, *7*, 2245–2253.
(38) Graser, F.; Hädicke, E. *Liebigs Ann. Chem.* **1980**, 1994–2011.
(39) Datar, A.; Balakrishnan, K.; Yang, X. M.; Zuo, X.; Huang, J. L.; Yen, M.; Zhao, J.; Tiede, D. M.; Zang, L. *J. Phys. Chem. B* **2006**, *110*, 12327–12332.
(40) Yang, X.; Xu, X.; Ji, H. *J. Phys. Chem. B* **2008**, *112*, 7196–7202.